Progress In Electromagnetics Research, PIER 25, 111–129, 2000

RECTANGULAR CONDUCTING WAVEGUIDE FILLED WITH UNIAXIAL ANISOTROPIC MEDIA: A MODAL ANALYSIS AND DYADIC GREEN'S FUNCTION

S. Liu, L. W. Li, M. S. Leong, and T. S. Yeo

Communications and Microwave Division
Department of Electrical Engineering
The National University of Singapore
Singapore 119260

1. INTRODUCTION

A general anisotropic medium is charaterized by permittivity tensor $\overline{\boldsymbol{\epsilon}}$ and permeability tensor $\overline{\boldsymbol{\mu}}$ [1–3], whose form depends on the kind of anisotropy. At present, different anisotropic materials are widely used in integrated optics and microwave engineering [4–8]. The technology advances are making the production of substrates, dielectric anisotropic films and anisotropic material filling more and more convenient. It shows the necessity of better charaterizing the anisotropic media and producing more realistic models for the components that use them.

Due to the complexity caused by the parameter tensors, the plane wave expansion is often used in the analysis of anisotropic media. And consequently, the Fourier transform is widely applied [1–3, 6, 9, 10] and will also be employed in this study. Using these methods, *Uzunoglu et* *al.* [9] found the solution of the vector wave equation in cylindrical coordinates for a gyroelectric medium. *Ren* [10] furthered the work under spherical coordinates in a similar procedure and obtained spherical wave functions and dyadic Green's functions in gyroelectric media. Recently, the theory of TE- and TM-decomposition attracts the interests of some researchers [11–13]. The TE- and TM-field decomposition is a method for solving electromagnetic problems involving certain class of boundaries and media that separate the field into reversely-handed circularly polarized waves. It is now extended to the problems of general uniaxially anisotropic media [11] and bi-anisotropic media [12, 13] from that of isotropic media.

In this paper, the fields in a rectangular conducting waveguide filled with a uniaxially anisotropic material are studied. The characteristic feature of the uniaxial media is the existence of a distinguished axis. If one of the coordinate axes is chosen to be parallel to this distinguished direction, it turns out that the parameter tensor is diagonal but the element referring to the distinguished axis is different from the remaining two diagonal ones. Some features of the waveguides of uniaxial anisotropic material have been analyzed and their applications made by some authors [4, 7, 8]. It's found in our study that the fields in a rectangular conducting waveguide filled with uniaxially anisotropic material are split into TE and TM modes after solving the eigenvalue equation. The calculated dispersion curves are then depicted. There exist considerable effects of the material parameters on the cutoff frequencies of the propagating waves, especially the TM modes. The dyadic Green's functions for various kinds of anisotropic media with different structures have been studied by many authors [14–20]. The problems, however, are mostly analyzed in spectral domain in terms of Fourier transform, due to the difficulty of finding the expansion of the dyadic Green's functions in terms of vector wave functions for anisotropic media. So far as we know, the dyadic Green's functions for anisotropic media-filled waveguides with perfectly conducting walls have not been shown in any literature. In our study, the suitable vector wave functions can be selected separately for the TE modes and TM modes by applying the boundary conditions. The dyadic Green's functions are then derived using *Ohm-Rayleigh method* [21]. It's shown that the expression obtained here is reducible to the isotropic case which has been obtained by *Tai* [21]. The magnetic type dyadic Green's function due to electric source can be obtained from the

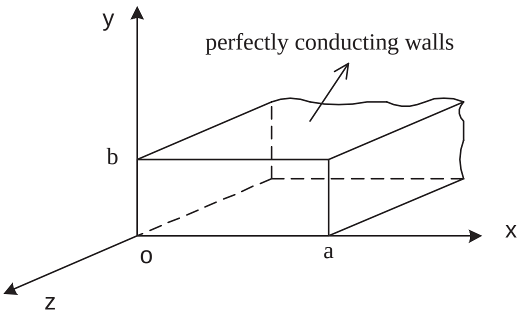

Figure 1. Geometry of a rectangular waveguide.

electric type one. As the application of the dyadic Green's function, numerical results of the the modes excited by an infinitesimal electric dipole are also given.

Throughout this paper, the harmonic $e^{-i\omega t}$ time dependence is assumed and suppressed. Bold prints indicate vectors and an overhead bold face indicates a dyad(ic). Caps with bold face represent unit vectors.

2. BASIC FORMULATION OF THE PROBLEM

Consider a rectangular waveguide (Fig. 1) of which coordinates axis system is represented by (x, y, z). $\widehat{\boldsymbol{z}}$ is the direction of propagation.

The waveguide is filled with homogeneous electrically uniaxial anisotropic medium that is characterized by the following set of constitutive relations:

$$\boldsymbol{D} = \epsilon_0 \overline{\boldsymbol{\epsilon}}_r \cdot \boldsymbol{E}, \tag{1a}$$

$$\boldsymbol{B} = \mu_0 \boldsymbol{H}, \tag{1b}$$

where ϵ_0 and μ_0 are the free space permittivity and permeability, respectively.

We assume that the optics axis of the uniaxial media is oriented along the $\boldsymbol{z}$-axis, and the other two principal axes are oriented along the two remaining coordinate axes. So the permitivity tensors $\overline{\boldsymbol{\epsilon}}_r$ is given by

$$\overline{\boldsymbol{\epsilon}}_r = \begin{bmatrix} \epsilon_t & 0 & 0 \\ 0 & \epsilon_t & 0 \\ 0 & 0 & \epsilon_z \end{bmatrix}. \tag{2}$$

It can be proved that $\overline{\boldsymbol{\epsilon}}_r$ takes the same form in both Cartesian and cylindrical coordinates systems. For this kind of media, the source-incorporated Maxwell's equations are written as

$$\nabla \times \boldsymbol{E} = i\omega\mu_0 \boldsymbol{H}, \tag{3b}$$

$$\nabla \times \boldsymbol{H} = -i\omega\epsilon_0 \overline{\boldsymbol{\epsilon}}_r \cdot \boldsymbol{E} + \boldsymbol{J}. \tag{3b}$$

Substituting (3a) into (3b) yields

$$\nabla \times \nabla \times \boldsymbol{E} - k_0^2 \overline{\boldsymbol{\epsilon}}_r \cdot \boldsymbol{E} = i\omega\mu_0 \cdot \boldsymbol{J}, \tag{4}$$

where $k_0 = \omega\sqrt{\epsilon_0\mu_0}$, which is the free space wavenumber.

3. FIELDS IN SOURCE-FREE RECTANGULAR WAVEGUIDE

Now we study the eigenvalues and eigenvectors of the source-free vector wave equation in an infinite uniaxial anisotropic medium. Let $\boldsymbol{J} = 0$, (4) reduces to

$$\nabla \times \nabla \times \boldsymbol{E} - k_0^2 \overline{\boldsymbol{\epsilon}}_r \cdot \boldsymbol{E} = 0. \tag{5}$$

The characteristic waves corresponding to (5) can be examined in the spectral domain using Fourier transform

$$\boldsymbol{E}(\boldsymbol{r}) = \iiint_{-\infty}^{+\infty} \boldsymbol{E}(\boldsymbol{k}) e^{i\boldsymbol{k}\cdot\boldsymbol{r}} d\boldsymbol{k} \tag{6}$$

where $\boldsymbol{k} = k_x\widehat{\boldsymbol{x}} + k_y\widehat{\boldsymbol{y}} + k_z\widehat{\boldsymbol{z}}$. Substituting (6) to (5), we have

$$\iiint_{-\infty}^{+\infty} (k^2\overline{\boldsymbol{I}} - \boldsymbol{kk} - k_0^2\overline{\boldsymbol{\epsilon}}_r) \cdot \boldsymbol{E}(\boldsymbol{k}) e^{i\boldsymbol{k}\cdot\boldsymbol{r}} d\boldsymbol{k} = 0 \tag{7}$$

where $\overline{\boldsymbol{I}} = \widehat{\boldsymbol{x}}\widehat{\boldsymbol{x}} + \widehat{\boldsymbol{y}}\widehat{\boldsymbol{y}} + \widehat{\boldsymbol{z}}\widehat{\boldsymbol{z}}$ is the unit dyadic. For nontrivial solutions of (7), it is required that the determinant of matrix $(k^2\overline{\boldsymbol{I}} - \boldsymbol{kk} - k_0^2\overline{\boldsymbol{\epsilon}}_r)$ must be equal to zero. Performing the algebraic operations, we obtain the characteristic equation finally as

$$\epsilon_t k_c^4 + (\epsilon_t + \epsilon_z)\left(k_z^2 - k_0^2\epsilon_t\right)k_c^2 + \epsilon_z\left(k_z^2 - k_0^2\epsilon_t\right)^2 = 0 \tag{8}$$

where $k_c^2 = k_x^2 + k_y^2$. Solving the characteristic equation, we have the eigenvalues given by

$$k_{c1}^2 = k_0^2\epsilon_t - k_z^2, \tag{9a}$$

$$k_{c2}^2 = k_0^2\epsilon_z - k_z^2\frac{\epsilon_z}{\epsilon_t}. \tag{9b}$$

It can be seen that k_{c1} is independent upon ϵ_z while k_{c2} is a function of ϵ_z, which lead to the ordinary and extraordinary waves [1], respectively. To find the corresponding eigenvectors, we substitute these eigenvalues back to (7). Finally we have

$$\begin{aligned} &E_{1z} = 0, \\ &E_{1x}\cos(\phi_k) + E_{1y}\sin(\phi_k) = 0, \\ &\boldsymbol{E}_1(\phi_k, k_z) = E_{1x}\widehat{\boldsymbol{x}} + E_{1y}\widehat{\boldsymbol{y}}, \end{aligned} \tag{10a}$$

for k_{c1}; and

$$\begin{aligned} &E_{2x} = A(k_z)\cos(\phi_k)E_{2z}, \\ &E_{2y} = A(k_z)\sin(\phi_k)E_{2z}, \\ &\boldsymbol{E}_2(\phi_k, k_z) = E_{2x}\widehat{\boldsymbol{x}} + E_{2y}\widehat{\boldsymbol{y}} + E_{2z}\widehat{\boldsymbol{z}}, \end{aligned} \tag{10b}$$

for k_{c2}; where

$$A(k_z) = \frac{\epsilon_z k_z}{\epsilon_t\sqrt{\epsilon_z(k_0^2 - k_z^2/\epsilon_t)}} \tag{10c}$$

and

$$\phi_k = \tan^{-1}(k_y/k_x). \tag{10d}$$

Obviously $\boldsymbol{E}_1$ takes TE modes, which can be expressed using the vector wave function $\boldsymbol{M}$ with $\widehat{\boldsymbol{z}}$ as the piloting vector [21]. In the Cartesian coordinate system, E_{2z} takes the form of $e^{j(k_{x2}x+k_{y2}y+k_z z)}$. From (3a) we have

$$H_{2z} = \frac{1}{i\omega\mu_0}\left[\frac{\partial(\boldsymbol{E}_2\cdot\widehat{\boldsymbol{y}})}{\partial x} - \frac{\partial(\boldsymbol{E}_2\cdot\widehat{\boldsymbol{x}})}{\partial y}\right] = 0, \tag{11}$$

which means $\boldsymbol{E}_2$ takes TM modes. So $\boldsymbol{E}_2$ can be expanded using vector wave function $\boldsymbol{N}$, and $\boldsymbol{L}$ with $\widehat{\boldsymbol{z}}$ as the piloting vector as well. For rectangular waveguides bounded at $x = 0$ and a and at $y = 0$ and b by conducting walls, these vector wave functions can be written as [21]

$$\boldsymbol{M}_{1{}^e_o}(h) = \boldsymbol{\nabla}\times\left(\begin{matrix}\cos\\ \sin\end{matrix} k_{x1}x \begin{matrix}\cos\\ \sin\end{matrix} k_{y1}y e^{jk_z z}\widehat{\boldsymbol{z}}\right), \tag{12a}$$

$$\boldsymbol{N}_{2{}^e_o}(h) = \frac{1}{k_2}\boldsymbol{\nabla}\times\boldsymbol{\nabla}\times\left(\begin{matrix}\cos\\ \sin\end{matrix} k_{x2}x \begin{matrix}\cos\\ \sin\end{matrix} k_{y2}y e^{jk_z z}\widehat{\boldsymbol{z}}\right), \tag{12b}$$

$$\boldsymbol{L}_{2{}^e_o}(h) = \boldsymbol{\nabla}\left(\begin{matrix}\cos\\ \sin\end{matrix} k_{x2}x \begin{matrix}\cos\\ \sin\end{matrix} k_{y2}y e^{jk_z z}\right). \tag{12c}$$

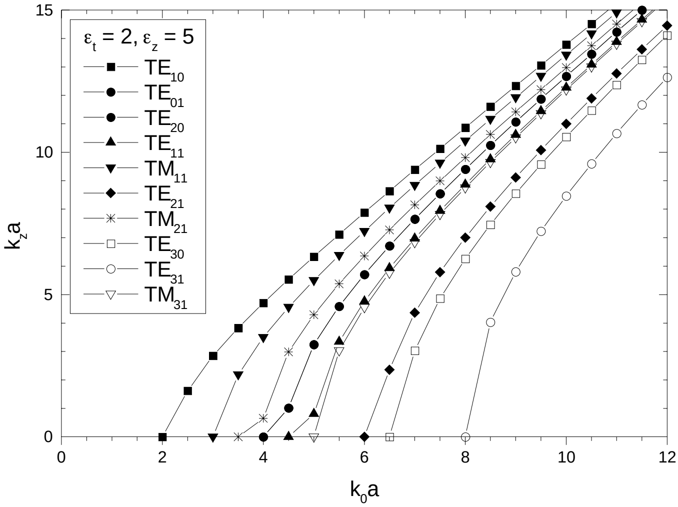

Figure 2. Dispersion curves for the lowest 10 modes.

It has been shown that fields can be decomposed into TE and TM modes. The observation is in agreement with Lindell's analysis [11] that decomposition method is applicable to such problems with perfect electric or magnetic conducting surfaces parallel to the $\boldsymbol{z}$-axis.

To match the boundary condition,

$$\widehat{\boldsymbol{z}} \cdot \boldsymbol{E}_2(\boldsymbol{r})|_{\text{boundary}} = 0 \tag{13}$$

must be satisfied, because E_{1z} is zero everywhere. (13) straightforwardly leads to that we should choose $\boldsymbol{N}_{2o}$ and $\boldsymbol{L}_{2o}$ as eigenfunctions of $\boldsymbol{E}_2(\boldsymbol{r})$, and that

$$k_{x2} = m_2\pi/a, \qquad m_2 = 1, 2, \cdots; \tag{14a}$$

$$k_{y2} = n_2\pi/b, \qquad n_2 = 0, 1, 2, \cdots. \tag{14b}$$

In this case, $\widehat{\boldsymbol{x}} \cdot \boldsymbol{E}_2(\boldsymbol{r})|_{\text{boundary}} = 0$ is automatically satisfied. So on the boundary, $\boldsymbol{E}_1(\boldsymbol{r})$ must satisfy

$$\widehat{\boldsymbol{x}} \cdot \boldsymbol{E}_1(\boldsymbol{r})|_{\text{boundary}} = 0, \tag{15}$$

which leads to that only $\boldsymbol{M}_{1e}$ can be chosen to represent $\boldsymbol{E}_1(\boldsymbol{r})$, and

$$k_{x1} = m_1\pi/a, \qquad m_1 = 1, 2, \cdots; \tag{16a}$$

$$k_{y1} = n_1\pi/b, \qquad n_1 = 0, 1, 2, \cdots. \tag{16b}$$

Equations (14) and (16), together with (9), make the dispersion relations for a rectangular conducting waveguide filled with a uniaxial anisotropic material. The calculated dispersion curves for $\epsilon_z/\epsilon_t = 2.5$ are depicted in Fig. 2 where $a/b = 2$. Only the modes corresponding to the lowest 10 modes (which are listed in sequence in the legend of Fig. 2) of an isotropic rectangular waveguide are shown. It is found that due to the existence of the optics axis, the order of these modes changes for the uniaxial material parameters. For example, TM_{11} is the fifth lowest mode in isotropic rectangular waveguide with the dimension of $a/b = 2$, but it becomes the 2nd lowest one in uniaxial rectangular waveguide with the same dimension. This phenomenon suggests that we can select the propagating mode we want by changing the material parameters. Since the optics axis of the uniaxial media only affects the TM modes in the present case, in Fig. 3 the cutoff frequencies of some TM modes are shown as ϵ_z increases from 1.0 to 10.0 $(\epsilon_t = 2.0)$. It can be seen that the cutoff frequencies monotonically decrease as ϵ_z increases.

In Fig. 4–6, some lowest TM modes are plotted for a uniaxial $(\epsilon_z/\epsilon_t = 2.5)$ rectangular waveguide and an isotropic $(\epsilon_z/\epsilon_t = 1.0)$ rectangular waveguide. The dimensions of the waveguide are selected so that $a/b = 2$. It can be seen that due to the existence of the optics axis, the distributions of the field intensity in the uniaxial waveguide are different from the isotropic ones. A greater ϵ_z produces more significant variation of the intensity distribution.

4. DYADIC GREEN'S FUNCTIONS

In this section, we perform the eigenfunction expansion of dyadic Green's functions for a rectangular waveguide filled with uniaxial material making use of the Ohm-Rayleigh method.

Consider an electric source $\boldsymbol{J}$ expressed in terms of the Dirac-delta function $\delta(\boldsymbol{r}-\boldsymbol{r}')$ and the unit dyadic $\overline{\boldsymbol{I}}$ as follow:

$$\boldsymbol{J}(\boldsymbol{r}) = \int_{V'} \delta(\boldsymbol{r}-\boldsymbol{r}')\overline{I}\cdot\boldsymbol{J}(\boldsymbol{r}')dV'. \tag{17}$$

Due to the linearity of (4), the electric field can be related directly to the source [21] through

$$\boldsymbol{E}(\boldsymbol{r}) = i\omega\mu_0 \int_{V'} \overline{\boldsymbol{G}}_{EJ}(\boldsymbol{r},\boldsymbol{r}')\cdot\boldsymbol{J}(\boldsymbol{r}')dV', \tag{18}$$

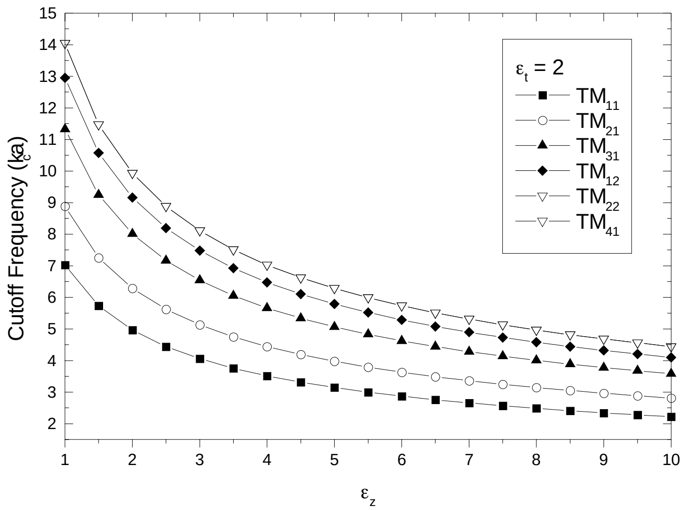

Figure 3. The cutoff frequencies for the lowest 6 TM-modes versus ϵ_z .

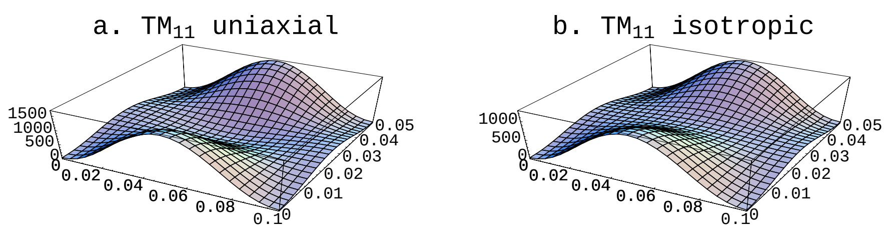

Figure 4. Electrical field intensities of TM_{11} mode.

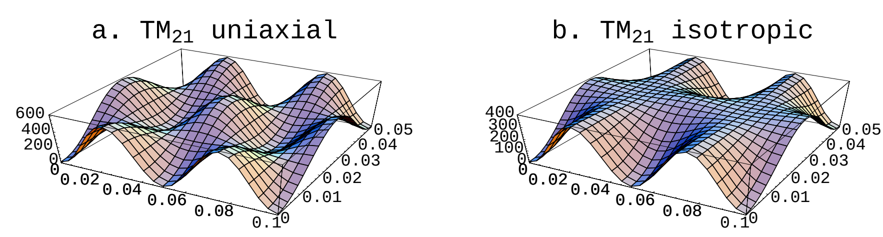

Figure 5. Electrical field intensities of TM_{21} mode.

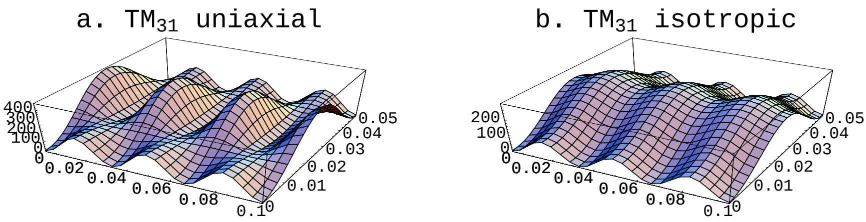

Figure 6. Electrical field intensities of TM_{31} mode.

where $\overline{\boldsymbol{G}}_{EJ}$ denotes electric dyadic Green function due to electric source, which is required to satisfy the dyadic Dirichlet condition $\widehat{\boldsymbol{n}} \times \overline{\boldsymbol{G}}_{EJ} = 0$ on the conducting boundaries, and V' stands for the volume occupied by the exciting current source. Substituting (17) and (18) into (4), we have

$$\boldsymbol{\nabla} \times \boldsymbol{\nabla} \times \overline{\boldsymbol{G}}_{EJ}(\boldsymbol{r}, \boldsymbol{r}') - k_0^2 \overline{\boldsymbol{\epsilon}}_r \cdot \overline{\boldsymbol{G}}_{EJ}(\boldsymbol{r}, \boldsymbol{r}') = \overline{\boldsymbol{I}} \delta(\boldsymbol{r} - \boldsymbol{r}'). \tag{19}$$

By inspection from the results of the previous section, $\overline{\boldsymbol{G}}_{EJ}$ can also be expanded using $\boldsymbol{M}_{1emn}$, $\boldsymbol{N}_{2omn}$ and $\boldsymbol{L}_{2omn}$ as

$$\begin{aligned}\overline{\boldsymbol{G}}_{EJ}(\boldsymbol{r}, \boldsymbol{r}') = \int_{-\infty}^{+\infty} dk_z \sum_{n,m} [&\boldsymbol{M}_{1emn}(k_z) \boldsymbol{a}_{1emn}(k_z) \\ &+ \boldsymbol{N}_{2omn}(k_z) \boldsymbol{b}_{2omn}(k_z) + \boldsymbol{L}_{2omn}(k_z) \boldsymbol{c}_{2omn}(k_z)]\end{aligned} \tag{20}$$

where $\boldsymbol{a}$, $\boldsymbol{b}$ and $\boldsymbol{c}$ are unknown coefficient matrices to be determined. (16) and (14) must be met to satisfy the boundary conditions. For convenience, we have used the notation mn to stand for m_1, n_1 and m_2, n_2 as well. Subsequently, we adopt the simplified notations $\boldsymbol{M}_{1e}$, $\boldsymbol{N}_{2o}$ and $\boldsymbol{L}_{2o}$ instead of $\boldsymbol{M}_{1emn}$, $\boldsymbol{N}_{2omn}$ and $\boldsymbol{L}_{2omn}$, respectively.

According to the Ohm-Rayleigh method we also expand the source function $\overline{\boldsymbol{I}} \delta(\boldsymbol{r} - \boldsymbol{r}')$, similarly, into

$$\begin{aligned}\overline{\boldsymbol{I}} \delta(\boldsymbol{r} - \boldsymbol{r}') = \int_{-\infty}^{+\infty} dk_z \sum_{n,m} [&\boldsymbol{M}_{1e}(k_z) \boldsymbol{P}_{1e}(k_z) \\ &+ \boldsymbol{N}_{2o}(k_z) \boldsymbol{Q}_{2o}(k_z) + \boldsymbol{L}_{2o}(k_z) \boldsymbol{V}_{2o}(k_z)].\end{aligned} \tag{21}$$

Taking the anterior scalar product of (21) with $\boldsymbol{M}_{1e'}(-k_z')$, $\boldsymbol{N}_{2o'}(-k_z')$, and $\boldsymbol{L}_{2o'}(-k_z')$ in turn and integrating the resultant equations through the entire volume of the rectangular waveguide, we can determine the coefficient matrices $\boldsymbol{P}$, $\boldsymbol{Q}$ and $\boldsymbol{V}$ given by

$$\boldsymbol{P}_{1e}(k_z) = \frac{2-\delta_0}{\pi ab k_{c1}^2}\boldsymbol{M}'_{1e}(-k_z), \tag{22a}$$

$$\boldsymbol{Q}_{2o}(k_z) = \frac{2-\delta_0}{\pi ab k_{c2}^2}\boldsymbol{N}'_{2o}(-k_z), \tag{22b}$$

$$\boldsymbol{V}_{2o}(k_z) = \frac{2-\delta_0}{\pi ab k_{2}^2}\boldsymbol{L}'_{2o}(-k_z). \tag{22c}$$

To obtain (22), the following orthogonality relations among the vector wave functions have been used, *i.e.*,

$$< \boldsymbol{M}_{1e}(k_z), \boldsymbol{M}_{1e'}(-k'_z) > = \frac{\pi ab k_{c1}^2}{2}(1+\delta_0)\delta_{mm'}\delta_{nn'}\delta(k_z - k'_z), \tag{23a}$$

$$< \boldsymbol{N}_{2o}(k_z), \boldsymbol{N}_{2o'}(-k'_z) > = \frac{\pi ab k_{c2}^2}{2}(1-\delta_0)\delta_{mm'}\delta_{nn'}\delta(k_z - k'_z), \tag{23b}$$

$$< \boldsymbol{L}_{2o}(k_z), \boldsymbol{L}_{2o'}(-k'_z) > = \frac{\pi ab k_{2}^2}{2}(1-\delta_0)\delta_{mm'}\delta_{nn'}\delta(k_z - k'_z), \tag{23c}$$

$$< \boldsymbol{M}_{1e}(k_z), \boldsymbol{N}_{2o'}(-k'_z) > = 0, \tag{23d}$$

$$< \boldsymbol{M}_{1e}(k_z), \boldsymbol{L}_{2o'}(-k'_z) > = 0, \tag{23e}$$

$$< \boldsymbol{N}_{2o}(k_z), \boldsymbol{L}_{2o'}(-k'_z) > = 0, \tag{23f}$$

where

$$\delta_0 = \begin{cases} 1, & m = 0 \text{ or } n = 0 \\ 0, & \text{otherwise} \end{cases},$$

$$\delta_{mm'} = \begin{cases} 1, & m = m' \\ 0, & m \neq m' \end{cases},$$

$$\delta_{nn'} = \begin{cases} 1, & n = n' \\ 0, & n \neq n' \end{cases}.$$

In (23), we've taken the operator $< \bullet, \bullet >$ [22] which defines

$$< \boldsymbol{a}, \boldsymbol{b} > = \iiint \boldsymbol{a} \cdot \boldsymbol{b} dV. \tag{24}$$

Substituting (20) and (21) into (19), and taking the anterior scalar product of (20) with $\boldsymbol{M}_{1e'}(-k'_z)$, $\boldsymbol{N}_{2o'}(-k'_z)$, and $\boldsymbol{L}_{2o'}(-k'_z)$ in the same way, we finally arrive at the following equation in matrix form:

$$[\Omega][X] = [\Theta], \tag{25}$$

where $[\Omega]$ is a 3×3 matrix given by

$$[\Omega] = \begin{bmatrix} \Omega_{11} & 0 & 0 \\ 0 & \Omega_{22} & \Omega_{23} \\ 0 & \Omega_{32} & \Omega_{33} \end{bmatrix}, \tag{26a}$$

with

$$\begin{aligned}
\Omega_{11} &= \frac{\pi ab}{2}(1+\delta_0)k_{c1}^2\left(k_1^2 - k_0^2\epsilon_t\right),\\
\Omega_{22} &= \frac{\pi ab}{2}(1-\delta_0)k_{c2}^2\left[k_2^2 - \frac{k_0^2}{k_2^2}\left(\epsilon_t k_z^2 + \epsilon_z k_{c2}^2\right)\right],\\
\Omega_{23} &= -\Omega_{32} = i\frac{\pi ab}{2}(1-\delta_0)\frac{k_z}{k_2}k_{c2}^2k_0^2(\epsilon_t - \epsilon_z),\\
\Omega_{33} &= -\frac{\pi ab}{2}(1-\delta_0)k_0^2\left(\epsilon_t k_{c2}^2 + \epsilon_z k_z^2\right).
\end{aligned}$$

In (26a), $[X]$ and $[\Theta]$ are two column vectors given by

$$[X] = \begin{bmatrix} \boldsymbol{a}_{1e}(k_z) \\ \boldsymbol{b}_{2o}(k_z) \\ \boldsymbol{c}_{2o}(k_z) \end{bmatrix}, \quad \text{and} \quad [\Theta] = \begin{bmatrix} \boldsymbol{M}'_{1e}(-k_z) \\ \boldsymbol{N}'_{2o}(-k_z) \\ \boldsymbol{L}'_{2o}(-k_z) \end{bmatrix}.$$

Solving (25), we have the solutions for $\boldsymbol{a}_{1e}(k_z)$, $\boldsymbol{b}_{2o}(k_z)$ and $\boldsymbol{c}_{2o}(k_z)$ as follows

$$\boldsymbol{a}_{1e}k_z) = \frac{2-\delta_0}{\pi abk_{c1}^2}\frac{1}{k_1^2 - k_{10}^2}\boldsymbol{M}_{1e}(-k_z), \tag{27a}$$

$$\boldsymbol{b}_{2o}(k_z) = \frac{2-\delta_0}{\pi abk_{c2}^2}\frac{1}{\epsilon_z k_2^2\left(k_2^2 - k_{20}^2\right)}\left[\beta_{NN}\boldsymbol{N}_{2o}(-k_z) + \beta_{NL}\boldsymbol{L}_{2o}(-k_z)\right], \tag{27b}$$

$$\boldsymbol{c}_{2o}(k_z) = \frac{2-\delta_0}{\pi abk_{c2}^2}\frac{1}{\epsilon_z k_2^2\left(k_2^2 - k_{20}^2\right)}\left[\beta_{LN}\boldsymbol{N}_{2o}(-k_z) + \beta_{LL}\boldsymbol{L}_{2o}(-k_z)\right], \tag{27c}$$

where the ordinary and extraordinary wave numbers are defined as

$$k_{10}^2 = k_0^2\epsilon_t, \tag{28a}$$

$$k_{20}^2 = k_0^2\epsilon_t + \left(1 - \frac{\epsilon_t}{\epsilon_z}\right)k_{c2}^2; \tag{28b}$$

and the coupling coefficients are given by

$$\beta_{NN} = \epsilon_t k_{c2}^2 + \epsilon_z k_z^2, \tag{28c}$$

$$\beta_{NL} = \frac{ik_z}{k_2} k_{c2}^2 (\epsilon_t - \epsilon_z), \tag{28d}$$

$$\beta_{LN} = -\frac{ik_z}{k_2} k_{c2}^2 (\epsilon_t - \epsilon_z), \tag{28e}$$

$$\beta_{LL} = -\frac{k_{c2}^2}{k_0^2 k_2^2} \left[k_2^4 - k_0^2 (\epsilon_t k_z^2 + \epsilon_z k_{c2}^2) \right]. \tag{28f}$$

Hence, (20) can be rewritten as

$$\begin{aligned} \overline{\boldsymbol{G}}_{EJ}(\boldsymbol{r}, \boldsymbol{r}') = \int_{-\infty}^{+\infty} dk_z \sum_{m,n} \Bigg\{ & \frac{2-\delta_0}{\pi ab k_{c1}^2} \frac{1}{k_1^2 - k_{10}^2} \boldsymbol{M}_{1e}(k_z) \boldsymbol{M}'_{1e}(-k_z) \\ & + \frac{2-\delta_0}{\pi ab k_{c2}^2} \frac{1}{\epsilon_z k_2^2 \left(k_2^2 - k_{20}^2\right)} \Big[\beta_{NN} \boldsymbol{N}_{2o}(k_z) \boldsymbol{N}'_{2o}(-k_z) \\ & + \beta_{NL} \boldsymbol{N}_{2o}(k_z) \boldsymbol{L}'_{2o}(-k_z) + \beta_{LN} \boldsymbol{L}_{2o}(-k_z) \boldsymbol{N}'_{2o}(-k_z) \\ & + \beta_{LL} \boldsymbol{L}_{2o}(k_z) \boldsymbol{L}'_{2o}(-k_z) \Big] \Bigg\}. \end{aligned} \tag{29}$$

In this way, the dyadic Green's functions for rectangular waveguides filled with uniaxial anisotropic media are explicitly represented in the form of the eigenfunction expansion in terms of the rectangular vector wave functions, as given in (29). However, for ease of practical applications and physical interpretation of possible novel phenomena, mathematical simplification to (29) is necessary. In order to apply the residue theorem to (20), we must first extract the irrotational term in (20) which does not satisfy the Jordan lemma as pointed out in [21]. To do so, we write

$$\boldsymbol{N}_{2o}(k_z) = \boldsymbol{N}_{2ot}(k_z) + \boldsymbol{N}_{2oz}(k_z), \tag{30a}$$

$$\boldsymbol{L}_{2o}(k_z) = \boldsymbol{L}_{2ot}(k_z) + \boldsymbol{L}_{2oz}(k_z), \tag{30b}$$

and so are $\boldsymbol{N}'$ and $\boldsymbol{L}'$. The subscripts t and z denote their transverse vector components and their $\boldsymbol{z}$-vector components respectively. In terms of these functions, (29) can be rewritten in the form

$$\overline{\boldsymbol{G}}_{EJ}(\boldsymbol{r}, \boldsymbol{r}') = \int_{-\infty}^{+\infty} dk_z \sum_{m,n} \Bigg\{ \frac{2-\delta_0}{\pi ab k_{c1}^2} \frac{1}{k_1^2 - k_{10}^2} \boldsymbol{M}_{1e}(k_z) \boldsymbol{M}'_{1e}(-k_z)$$

$$+\frac{2-\delta_0}{\pi abk_{c2}^2}\frac{1}{\epsilon_z k_2^2\left(k_2^2-k_{20}^2\right)}\left[\frac{k_0^2\epsilon_z-k_{c2}^2}{k_z^2}\boldsymbol{N}_{2ot}(k_z)\boldsymbol{N}'_{2ot}(-k_z)\right.$$
$$+\boldsymbol{N}_{2ot}(k_z)\boldsymbol{N}'_{2oz}(k_z)+\boldsymbol{N}_{2oz}(k_z)\boldsymbol{N}'_{2ot}(-k_z)$$
$$\left.\left.+\frac{k_0^2\epsilon_t-k_z^2}{k_{c2}^2}\boldsymbol{N}_{2oz}(k_z)\boldsymbol{N}'_{2oz}(k_z)\right]\right\}, \tag{31}$$

where we have expressed $\boldsymbol{L}_{2ot}(k_z)$ and $\boldsymbol{L}_{2oz}(k_z)$ in terms of $\boldsymbol{N}_{2ot}(k_z)$ and $\boldsymbol{N}_{2oz}(n,k_z)$, namely,

$$\boldsymbol{L}_{2ot}(k_z)=-\frac{ik_2}{k_z}\boldsymbol{N}_{2ot}(k_z), \tag{32a}$$

$$\boldsymbol{L}_{2oz}(k_z)=\frac{ik_zk_2}{k_{c2}^2}N_{2oz}(k_z), \tag{32b}$$

and similarly for the primed functions.

The singular term in (31) is contained in the component $\boldsymbol{N}_{2oz}(k_z)$ $\boldsymbol{N}'_{2oz}(-k_z)$ [21]. From (21), we note that

$$\widehat{\boldsymbol{z}}\widehat{\boldsymbol{z}}\delta(\boldsymbol{r}-\boldsymbol{r}')=\int_{-\infty}^{\infty}dk_z\sum_{m,n}\frac{2-\delta_0}{\pi ab}\left[\frac{1}{k_{c2}^2}\boldsymbol{N}_{2oz}(k_z)\boldsymbol{N}'_{2oz}(-k_z)\right.$$
$$\left.+\frac{1}{k_2^2}\boldsymbol{L}_{2oz}(k_z)\boldsymbol{L}'_{2oz}(-k_z)\right]$$
$$=\int_{-\infty}^{\infty}dk_z\sum_{m,n}\frac{2-\delta_0}{\pi abk_{c2}^2}\frac{k_2^2}{k_{c2}^2}\boldsymbol{N}_{2oz}(k_z)\boldsymbol{N}'_{2oz}(-k_z). \tag{33}$$

Making use of the identity

$$\frac{k_2^2}{k_0^2\epsilon_z\left(k_2^2-k_{20}^2\right)}\frac{k_0^2\epsilon_t-k_z^2}{k_{c2}^2}=-\frac{k_2^2}{k_0^2\epsilon_zk_{c2}^2}+\frac{\epsilon_tk_2^2}{k_0^2\epsilon_z^2\left(k_2^2-k_{20}^2\right)}, \tag{34}$$

we can split (31) into

$$\overline{\boldsymbol{G}}_{EJ}(\boldsymbol{r},\boldsymbol{r}')=-\int_{-\infty}^{\infty}dk_z\sum_{m,n}\frac{2-\delta_0}{\pi abk_{c2}^2}\frac{k_2^2}{k_0^2\epsilon_zk_{c2}^2}\boldsymbol{N}_{2oz}(k_z)\boldsymbol{N}'_{2oz}(-k_z)$$
$$+\int_{-\infty}^{+\infty}dk_z\sum_{m,n}\left\{\frac{2-\delta_0}{\pi abk_{c1}^2}\frac{1}{k_1^2-k_{10}^2}\boldsymbol{M}_{1e}(k_z)\boldsymbol{M}'_{1e}(-k_z)\right.$$
$$+\frac{2-\delta_0}{\pi abk_{c2}^2}\frac{k_2^2}{k_0^2\epsilon_z\left(k_2^2-k_{20}^2\right)}\left[\frac{k_0^2\epsilon_z-k_{c2}^2}{k_z^2}\boldsymbol{N}_{2ot}(k_z)\boldsymbol{N}'_{2ot}(-k_z)\right.$$
$$+\boldsymbol{N}_{2ot}(k_z)\boldsymbol{N}'_{2oz}(-k_z)+\boldsymbol{N}_{2oz}(k_z)\boldsymbol{N}'_{2ot}(-k_z)$$
$$\left.\left.+\frac{\epsilon_t}{\epsilon_z}\boldsymbol{N}_{2oz}(k_z)\boldsymbol{N}'_{2oz}(-k_z)\right]\right\}. \tag{35}$$

In view of (33), the first integral in (35) is equal to

$$-\frac{1}{k_0^2\epsilon_z}\widehat{\boldsymbol{z}}\widehat{\boldsymbol{z}}\delta(\boldsymbol{r}-\boldsymbol{r}'), \tag{36}$$

and the second integral can be evaluated by making use of the residue theorem in the k_z-plane. The final result is given after some mathematical manipulations by

$$\begin{aligned}\overline{\boldsymbol{G}}_{EJ}(\boldsymbol{r},\boldsymbol{r}') =& -\frac{1}{k_0^2\epsilon_z}\widehat{\boldsymbol{z}}\widehat{\boldsymbol{z}}\delta(\boldsymbol{r}-\boldsymbol{r}') + \frac{i}{ab}\sum_{m,n}\left\{\frac{1}{k_{c1}^2 k_{z1}}\boldsymbol{M}_{1e}(\pm k_{z1})\boldsymbol{M}'_{1e}(\mp k_{z1})\right.\\ &+\frac{k_{20}^2}{k_0^2\epsilon_t k_{c2}^2 k_{z2}}\left[\boldsymbol{N}_{2ot}(\pm k_{z2})+\frac{\epsilon_t}{\epsilon_z}\boldsymbol{N}_{2oz}(\mp k_{z2})\right]\\ &\left.\times\left[\boldsymbol{N}'_{2ot}(\mp k_{z2})+\frac{\epsilon_t}{\epsilon_z}\boldsymbol{N}'_{2oz}(\mp k_{z2})\right]\right\}, z \gtrless z'\end{aligned} \tag{37}$$

where z and z' are the positions of the observation point and the source point, respectively, measured along the $\widehat{\boldsymbol{z}}$-direction, and

$$k_{z1}^2 = k_{10}^2 - k_{c1}^2, \tag{38a}$$

$$k_{z2}^2 = k_{20}^2 - k_{c2}^2, \tag{38b}$$

with k_{10} and k_{20} having been defined in (28).

It can be observed that (37) is reducible to the isotropic case by assuming that $\epsilon_t = \epsilon_z = \epsilon$. In this case, $k_{10}^2 = k_{20}^2 = k_0^2\epsilon$ and (37) shall be simplified as:

$$\begin{aligned}\overline{\boldsymbol{G}}_{EJ}(\boldsymbol{r},\boldsymbol{r}') =& -\frac{1}{k_0^2\epsilon}\widehat{\boldsymbol{z}}\widehat{\boldsymbol{z}}\delta(\boldsymbol{r}-\boldsymbol{r}') + \frac{i}{ab}\sum_{m,n}\frac{2-\delta_0}{k_c^2 k_z}\Big[\boldsymbol{M}_e(\pm k_z)\boldsymbol{M}'_e(\mp k_z)\\ &+\boldsymbol{N}_o(\pm k_z)\boldsymbol{N}'_o(\mp k_z)\Big], \quad z \gtrless z'\end{aligned} \tag{39}$$

which is exactly the same as that obtained by Tai [21].

So far, we have obtained the electric dyadic Green's function as given in (37). With this electric DGF, the electric field can be obtained directly from (18). To obtain the magnetic field due to an electric current distribution, we need to utilize the following Maxwell's equation

$$\boldsymbol{\nabla}\times\boldsymbol{E} = i\omega\mu_0\boldsymbol{H}, \tag{40a}$$

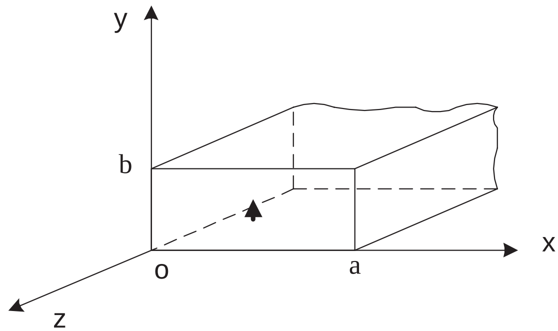

Figure 7. Excitation of an electric dipole.

or that in dyadics form

$$\nabla \times \overline{\boldsymbol{G}}_{EJ} = \overline{\boldsymbol{G}}_{HJ}. \tag{40b}$$

If we express the magnetic field in terms of the magnetic dyadic Green's function, we have the following integral:

$$\boldsymbol{H} = \iiint_{V'} \overline{\boldsymbol{G}}_{HJ}(\boldsymbol{r}, \boldsymbol{r}') \cdot \boldsymbol{J}(\boldsymbol{r}')dV'. \tag{41}$$

5. APPLICATION OF DYADIC GREEN'S FUNCTIONS

In this section, an infinitesimal dipole in $\widehat{\boldsymbol{y}}$-direction is assumed as the electric current source in the rectangular waveguide filled with uniaxial material. In a three-dimensional expression form, this source distribution is expressed by

$$\boldsymbol{J}(\boldsymbol{r}') = I_0 \widehat{\boldsymbol{y}} \delta(x' - x_0)\delta(y' - y_0)\delta(z' - z_0) \tag{42}$$

where the point (x', y', z') is located at the center of the rectangular waveguide cross section as shown in Fig. 7, *i.e.*,

$$x_0 = \frac{a}{2}, \quad y_0 = \frac{b}{2}, \quad z_0 = 0. \tag{43}$$

Substituting the above current distribution and (37) into (18), we have

$$\overline{\boldsymbol{E}}(\boldsymbol{r}) = -\frac{I_0\omega\mu_0}{ab}\sum_{m,n}\left\{\frac{k_{x1}}{k_{c1}^2 k_{z1}}\left[\sin\left(k_{x1}\frac{a}{2}\right)\cos\left(k_{y1}\frac{b}{2}\right)\right]\boldsymbol{M}_{1e}(\pm k_{z1})\right.$$
$$\pm\frac{ik_{20}^2 k_{y2}}{k_0^2\epsilon_t k_2 k_{c2}^2}\left[\sin\left(k_{x2}\frac{a}{2}\right)\cos\left(k_{y2}\frac{b}{2}\right)\right]\left[\boldsymbol{N}_{2ot}(\pm k_{z2})\right.$$
$$\left.\left.+\frac{\epsilon_t}{\epsilon_z}\boldsymbol{N}_{2oz}(\mp k_{z2})\right]\right\}, \qquad z \gtrless z'. \tag{44}$$

From (44), it is easy to find out that only the modes with odd m and even n are excited. Since for TE waves, a uniaxial medium with the optics axis in $\boldsymbol{z}$-direction looks like an isotropic medium, the fields of TE modes in the uniaxial anisotropic medium should have the same representations as the well-known ones in the isotropic medium. Therefore, we should discuss the features of the TM-mode fields only. In our subsequent numerical computation, the dimensions of the waveguide and the parameters of the material are selected as the same as those in the previous section ($i.e.$, $a/b = 2$, $\epsilon_t = 2.0$, and $\epsilon_z = 2.5$), for ease and meaningfulness of comparison. Fig. 8 and Fig. 9 show the electric field intensity and E_z distributions of TM_{12} mode and TM_{32} mode in the transverse cross-section. It is seen that the distribution of the guided TM modes in a uniaxial anisotropic medium has changed as compared with those guided ones in an isotropic medium.

6. CONCLUSION

The electromagnetic fields in rectangular conducting waveguides filled with uniaxial anisotropic media are characterized in this paper. With the optics axis of the uniaxial media oriented along the $\boldsymbol{z}$-axis of the waveguide, the fields can be decomposed into TE and TM modes with different propagation wave numbers. The ordinary wave takes the form of TE modes while the extraordinary wave takes the form of TM modes. The calculated dispersion curves are depicted and the effects of the material parameters on the cutoff frequencies are shown. The cutoff frequencies change considerably, especially for TM modes. The field distributions are drawn and compared with those in the isotropic rectangular waveguide. The electric type dyadic Green's function due to an electric source is derived by using eigenfunctions expansion and the Ohm-Rayleigh method. The irrotational term is properly extracted.

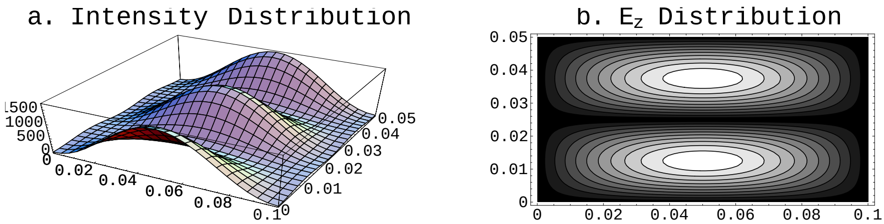

Figure 8. The distribution of TM_{12} mode in the transverse cross-section: (a) Electric field intensity and (b) E_z distribution.

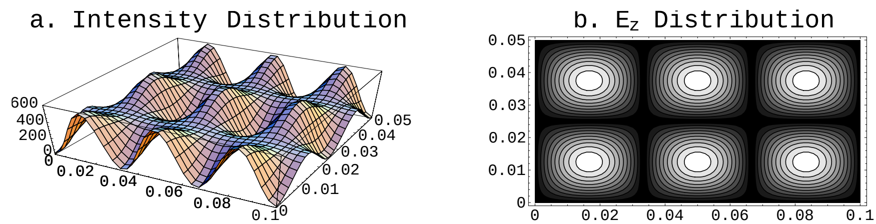

Figure 9. The distribution of TM_{32} mode in the transverse cross-section: (a) Electric field intensity and (b) E_z distribution.

It shows that the expression obtained can be readily reduced to that in the case of filled isotropic media. The magnetic type dyadic Green's function due to an electric source is also obtained from the electric one through Maxwell equations. As an application of the dyadic Green's function, numerical results of the the modes excited by an infinitesimal electric dipole are presented and discussed.

ACKNOWLEDGMENT

This project is supported in part by the Ministry of Education, Republic of Singapore by a research grant RP3981676.

REFERENCES

1. Chen, H. C., *Theory of Electromagnetic Waves*, McGraw-Hill, New York, 1983.
2. Kong, J. A., *Electromagnetic Wave Theory*, The 2nd ed., John Wiley & Sons, New York, 1986.

3. Chew, W. C., *Waves and Fields in Inhomogeneous Media*, Van Nostrand Reinhold, New York, 1990.
4. Singh, J., and K. Thyagarajan, "Analysis of metal clad uniaxial waveguides," *Optics Communications*, Vol. 85, 397–402, 1991.
5. Lu, M., and M. M. Fejer, "Anisotropic dielectric waveguides," *J. Opt. Soc. Am. A*, Vol. 10, No. 2, 246–261, Feb. 1993.
6. Toscano, A., and L. Vegni, "Spectral electromagnetic modeling of a planar integrated structure with a general grounded anisotropic slab," *IEEE Trans. Ant. Prop.*, Vol. 41, No. 3, 362–370, Mar. 1993.
7. Manenkov, A. B., "Orthogonality relations for the eigenmodes of lossy anisotropic waveguides (fibres)," *IEE Proceedings-J*, Vol. 140, No. 3, 206–212, June 1993.
8. Sawa, S., T. Kitamura, M. Geshiro, and T. Yoshikawa, "Low loss optical waveguide bends consisting of uniaxial crystalline material," *IEICE Trans. Electron.*, Vol. E78-C, No. 10, 1373–1377, Oct. 1995.
9. Uzunoglu, N. K., P. G. Cottis, and J. G. Fikioris, "Excitation of electromagnetic waves in a gyroelectric cylinder," *IEEE Trans. Ant. Propa.*, Vol. AP-33, No. 1, 90–99, Jan. 1985.
10. Ren, W., "Contributions to the electromagnetic wave theory of bounded homogeneous anisotropic media," *Physical Review E*, Vol. 47, No. 1, 664–673, Jan. 1993.
11. Lindell, I. V., "TE/TM decomposition of electromagnetic sources in uniaxial anisotropic media," *Microwave and Optical Tech. Lett.*, Vol. 9, No. 2, 108–111, June 1995.
12. Lindell, I. V., and F. Olyslager, "Decomposition of electromagentic sources in axially chiral uniaxial anisotropic media," *J. Electromagnetic Waves and Applications*, Vol. 10, No. 1, 51–59, 1996.
13. Lindell, I. V., "Decomposition of electromagnetic fields in bianisotropic media," *J. Electromagnetic Waves and Applications*, Vol. 11, No. 5, 645–657, 1997.
14. Lee, J. K., and J. A. Kong, "Dyadic Green's functions for layered anisotropic medium," *Electromagnetics*, Vol. 3, 111-130, 1983.
15. Weiglhofer, W. S., "Dyadic Greens functions for general uniaxial media," *IEE Proc. H.*, Vol. 137, No. 1, 5–10, Feb. 1990.
16. Weiglhofer, W. S., "A dyadic Green's function representation in electrically gyrotropic media," *AEÜ*, Vol. 47, No. 3, 125–130, 1993.
17. Barkeshli, S., "Electromagnetic dyadic Green's function for multilayered symmetric gyroelectric media," *Radio Science*, Vol. 28, No. 1, 23–36, Jan.-Feb. 1993.

18. Barkeshli, S., "An efficient asymptotic closed-form dyadic Green's function for grounded double-layered anisotropic uniaxial material slabs," *J. Electromagnetic Waves and Applications*, Vol. 7, No. 6, 833–856, 1993.
19. Cottis, P. G., and G. D. Kondylis, "Properties of the dyadic Green's function for an unbounded anisotropic medium," *IEEE Trans. Ant. Prop.*, Vol. 43, No. 2, 154–161, Feb. 1995.
20. Mudaliar, S., and J. K. Lee, "Dyadic Green's functions for a two-layer biaxially anisotropic medium," *J. Electromagnetic Waves and Applications*, Vol. 10, 909–923, 1996.
21. Tai, C. T., *Dyadic Green's Functions in Electromagnetic Theory*, The 2nd ed., IEEE Press, Piscataway, New Jersey, 1994.
22. Pearson, L. W., "On the spectral expansion of the electric and magnetic dyadic Greens functions in cylindrical harmonics", *Radio Science*, Vol. 18, No. 2, 166–174, March–April 1983.